Structural Engineering and Mechanics, *Vol. 54, No. 3 (2015) 579-595*
DOI: http://dx.doi.org/10.12989/sem.2015.54.3.579

Investigation of the Instability of FGM box beams

Noureddine Ziane*[1], Sid Ahmed Meftah[1], Giuseppe Ruta[2], Abdelouahed Tounsi[3] and El Abbas Adda Bedia[3]

[1]Laboratoire des Structures et Matériaux Avancés dans le Génie Civil et Travaux Publics, Université de Djillali Liabes, Sidi Bel Abbes, Algeria
[2]Department of Structural & Geotechnical Engineering. Faculty of Civil & Industrial Engineering, Sapienza University, Rome, Italy
[3]Laboratoire des Matériaux et Hydrologie, Université de Sidi Bel Abbes, Algérie

(Received January 30, 2015, Revised March 23, 2015, Accepted March 24, 2015)

Abstract. A general geometrically non-linear model for lateral-torsional buckling of thick and thin-walled FGM box beams is presented. In this model primary and secondary torsional warping and shear effects are taken into account. The coupled equilibrium equations obtained from Galerkin's method are derived and the corresponding tangent matrix is used to compute the critical moments. General expression is derived for the lateral-torsional buckling load of unshearable FGM beams. The results are validated by comparison with a 3D finite element simulation using the code ABAQUS. The influences of the geometrical characteristics and the shear effects on the buckling loads are demonstrated through several case studies.

Keywords: lateral torsional buckling; box beam; FGM; non-linear; Galerkin's method

1. Introduction

Thick and thin-walled box elements with composite materials are widely used in engineering applications like aircraft wings, helicopter rotor blades, robot arms, bridge decks and other structural elements in civil constructions. However, in contrast to the steel box beams, the composite ones offer competitive solutions to achieve a structural weight reduction and a good bending-twist resistance. In addition, the material, the beam length, the load height and the cross-section parameter can play an important role on the lateral-torsional buckling behavior of such structures. The problem of the constrained torsion of isotropic closed-section thin-walled beams was addressed in the pioneering works by Vlasov (1962) and Gjelsvik (1981). Vlasov's theory is also used to develop a thin-walled beam model by Fu and Hsu (1995). Kim and Kim (1999) have developed a one-dimensional beam theory to deal with coupled deformations of torsion, warping and distortion in thin-walled general sectioned beams. These investigations have addressed the significant effects of distortion and warping deformations on the analysis accuracy.

Paulsen and Welo (2001) have also shown the effect of the hour-glass section distortion on the buckling phenomena of hollow rectangular beams. While there is a considerable body of literature

*Corresponding author, Ph.D., E-mail: zianenoureddine@yahoo.fr

http://www.techno-press.org/?journal=sem&subpage=8 ISSN: 1225-4568 (Print), 1598-6217 (Online)

available on the stability of thin-walled metallic structures (see for example Ruta *et al*. 2008, Pignataro *et al*. 2010, Erkmen and Attard 2011, Gonçalves 2012, Lofrano *et al*. 2013, Erkmen 2014), the corresponding studies on composite structures are rather few. Moreover, these studies have been confined only to open cross-section beams. Fraternali and Feo (2000) used a finite element formulation by generalizing the classical Vlasov theory of sectorial areas and without considering shear deformation to solve the problem of non-linear stability of thin-walled composite beams with open cross-section. Sapkàs and kollàr (2002) presented stability analysis of simply supported and cantilever composite thin-walled beams with open section subjected to three different load conditions, the Ritz method was applied to derive their closed form approximate solution for the buckling load. Subsequently, Machado and Cortínez (2005a, b) developed a geometrically non-linear theory based on the assumptions adopted by Cortínez and Piovan (2002) to study the lateral-torsional buckling behavior of composite bisymmetric open and closed cross-sections thin-walled beams, the Ritz method was applied in order to obtain an approximate tangential matrix that allows to determine the critical loads considering prebuckling deflections, effects of shear flexibility were investigated with numerical results. Based on the power series expansions of displacement components, an element stiffness matrix for the spatially coupled stability analysis of thin-walled composite beam with symmetric and non-symmetric laminations has been presented by Kim *et al*. (2008), their numerical solutions have been compared with analytical and finite element results. However, the use of the composite materials was limited by the high temperature until the appearance of new material known as functionally graded material (FGM). Microscopically the FGM is non-homogeneous but at macro level, the mechanical properties vary continuously from one surface to another by smoothly varying the volume fractions of the material constituents. It is noted that, FGMs have received wide applications in modern industries including aerospace, mechanical, electronics, optics, chemical, biomedical, nuclear, and civil engineering to name a few during the past two decades (Bouderba *et al*. 2013, Tounsi *et al*. 2013, Belabed *et al*. 2014, Ait Amar Meziane *et al*. 2014, Fekrar *et al*. 2014, Bousahla *et al*. 2014, Khalfi *et al*. 2014, Hebali *et al*. 2014, Zidi *et al*. 2014, Al-Basyouni *et al*. 2015, Bourada *et al*. 2015, Ait Yahia *et al*. 2015). Reviewing the literature on FG materials, it is understood that the literature is mostly dedicated to stability analysis of cylindrical shells and very few research works have been carried out on FGM box beams. Shen (2009) and later Dung and Hoa (2013) investigated the buckling and post-buckling of imperfect cylindrical shells subjected to torsion based on the von Karman–Donnell-type non-linear differential equations. The more recent work on the study of the buckling of thin-walled box beams made of FGM have been carried out by Lanc *et al*. (2015), they adopted a non-linear displacement field to investigate effects of the power-law index and skin-core-skin thickness ratios on the critical buckling loads and post-buckling responses but the shear effects across the wall-thickness was neglected, therefore, the primary purpose of the current work is to fill this gap for studying the lateral-torsional buckling of thick and thin-walled FGM box beams. To this end, the considered structure is modeled by introducing the function used by Reddy (1984) satisfying the shear-stress-free boundary conditions at top, bottom, left, and right of the cross section in non-linear displacement fields. The solution of the equilibrium equations are derived via Galerkin Method and the critical moment are obtained by requiring the singularity of the tangential matrix with the linear bending problem. Finally, in order to put into evidence the effects of transverse shear, three models results are presented in the case of simply supported box beams under uniformly distributed loads.

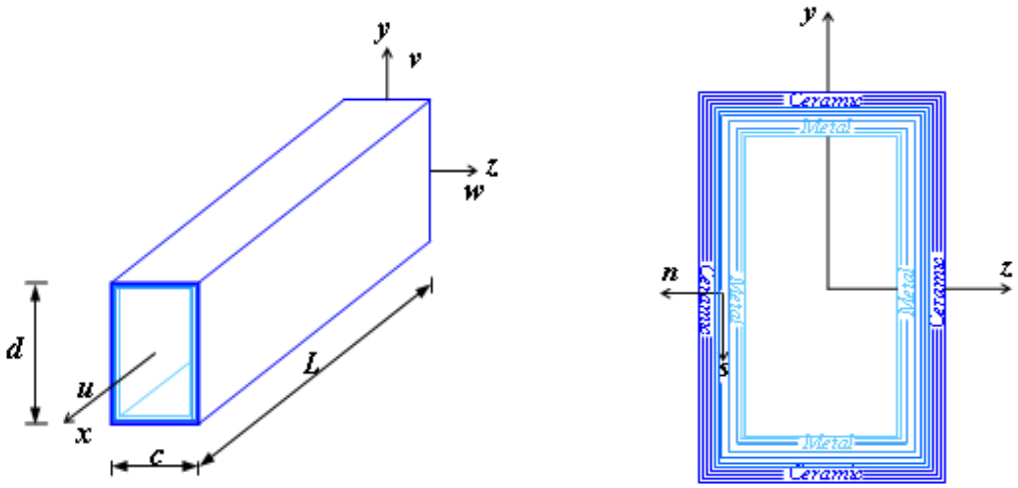

(a) (b)

Fig. 1 Geometry and material variation of the FGM box beam

2. Kinematics

Consider a symmetric FGM box beam of length L, minimum cross-sectional dimension c, maximum cross-sectional dimension d and wall thickness h (see Fig. 1). The Cartesian coordinate system (x, y, z) and the curvilinear system (x, s, n) are used. The coordinate s is measured along the tangent to the middle surface in a counter-clockwise direction, while n is the coordinate perpendicular to the s coordinate. The origin of the coordinates is set at the center of beam cross-section.

It is assumed that the Young's modulus of FGM beam (Eq. (1)) varies through the wall-thickness according to power law form used by Wakashima *et al*. (1990).

$$E(n)= (E_t - E_b)[(n/h)+(1/2)]^p + E_b \tag{1}$$

Where E_t and E_b denote values of the elasticity modulus at $n=h/2$ and $n=-h/2$, respectively and p is a variable parameter which dictates the material variation profile through the thickness.

To develop the present model, a number of assumptions are stipulated:

(a) The beam cross-sections are assumed rigid in their own planes.

(b) Transverse shear stresses vary parabolically across the minimum and maximum cross-sectional dimensions.

(c) Torsional primary and secondary warping are included in this formulation.

(d) The Poisson's coefficient ν is assumed to be constant.

In general, the displacements, u, v and w of any generic point on the profile section in the x, y and z directions, respectively, may be expressed as

$$u = u_0 - y(v_0'cos\theta + w_0'sin\theta) - z(w_0'cos\theta - v_0'sin\theta) - \psi\theta'$$
$$+(f(y)\left(v_0' - \phi_y\right) + f(z)\left(w_0' - \phi_z\right))cos\theta + (f(y)\left(w_0' - \phi_z\right) - f(z)\left(v_0' - \phi_y\right))sin\theta \tag{2a}$$

$$v = v_0 - zsin\theta - y(1 - cos\theta) \tag{2b}$$

$$w = w_0 + y\sin\theta - z(1 - \cos\theta) \tag{2c}$$

Where u_0, v_0 and w_0 are the mid-plane displacements in the x, y, and z directions, while the variables ϕ_y, ϕ_z and θ denote the rotations about the z, y and x axes, respectively. The superscript primes denote the partial derivatives with respect to x.

The primary and secondary torsional warping functions ψ_p and ψ_s are replaced by that of Sokolnikoff (1946) in Eq. (3).

$$\psi(y,z) = \psi_p(y,z) + \psi_s(y,z) = -yz + \frac{8d^2}{\pi^3}\sum_{i=0}^{\infty}\frac{\sin\left(\frac{(2i+1)\pi y}{d}\right)\sinh\left(\frac{(2i+1)\pi z}{d}\right)\sin\left(\frac{(2i+1)\pi}{2}\right)}{(2i+1)^3\cosh\left(\frac{(2i+1)\pi c}{2d}\right)} \tag{3}$$

Whereas, $f(y)$ and $f(z)$ represent the shape functions determining the distribution of the transverse shear strain and stress through the minimum and maximum cross-sectional dimensions. By choosing appropriate $f(y)$ and $f(z)$ terms, different well known models could be expressed:

- $Model(I)$: $\begin{cases} f(y) = y - \frac{4y^3}{3d^2} \\ f(z) = z - \frac{4z^3}{3c^2} \end{cases}$
- $Model(II)$: $\begin{cases} f(y) = y \\ f(z) = z \end{cases}$
- $Model(III)$: $\begin{cases} f(y) = 0 \\ f(z) = 0 \end{cases}$

The functions introduced by Reddy (1984) satisfying the shear-stress-free boundary conditions is used in the case of model (I). The model (II) is mainly based on constant transverse shear stresses through the cross-sectional dimensions. In model (III), deformations due to the transverse shear are neglected.

Let us recall that the kinematic equations (Mohri *et al*. 2002) can be obtained from Eq. (2) by using the model (III). Moreover, the displacement field used by Ziane *et al*. (2013) is obtained from the model (II) by using the approximation $\cos\theta=1$ and $\sin\theta=\theta$ and by disregarding the resulting non-linear terms.

Thus, for Model (I), the expression in Eq. (2) is a generalization of others previously proposed in the literature.

In the case of thin and thick box beams, the components of Green's strain tensor which incorporate the large displacements are reduced to the following one:

$$\varepsilon_{ij} = \frac{1}{2}\left(\frac{\partial u_i}{\partial x_j} + \frac{\partial u_j}{\partial x_i} + \left(\frac{\partial u_k}{\partial x_i}\frac{\partial u_k}{\partial x_j}\right)\right) \tag{4}$$

Substituting Eq. (2) into Eq. (4) one obtain the components of the strain tensor which can be expressed in the following form

$$\varepsilon_{xx} = u_0' - y\left(v_0'' \cos(\theta) + w_0'' \sin(\theta)\right) - z\left(w_0'' \cos(\theta) - v_0'' \sin(\theta)\right) - \psi\theta''$$
$$+f(y)\left(\left(v_0'' - \phi_y'\right)\cos(\theta) - \theta'\left(v_0' - \phi_y\right)\sin(\theta) + \left(w_0'' - \phi_z'\right)\sin(\theta) + \theta'\left(w_0' - \phi_z\right)\cos(\theta)\right)$$
$$+f(z)\left(\left(w_0'' - \phi_z'\right)\cos(\theta) - \theta'\left(w_0' - \phi_z\right)\sin(\theta) - \left(v_0'' - \phi_y'\right)\sin(\theta) - \theta'\left(v_0' - \phi_y\right)\cos(\theta)\right)$$
$$+\frac{1}{2}\left(v_0'^2 + w_0'^2 + (y^2 + z^2)\theta'^2\right) \tag{5a}$$

$$\gamma_{xy} = \frac{df(y)}{dy}\left(\left(v_0' - \phi_y\right)\cos(\theta) + \left(w_0' - \phi_z\right)\sin(\theta)\right) - \left(z + \frac{\partial \psi}{\partial y}\right)\theta' \tag{5b}$$

$$\gamma_{xz} = \frac{df(z)}{dz}\left(\left(w_0' - \phi_z\right)\cos(\theta) - \left(v_0' - \phi_y\right)\sin(\theta)\right) - \left(\frac{\partial \psi}{\partial z} - y\right)\theta' \tag{5c}$$

Hooke's law for FGM beam walls in the global coordinate system for the flanges are obtained by replacing the subscripts *s* and *n* in Eq. (6) by *y* and *z*, respectively, whereas *s* and *n* are replaced by *z* and *y* for the webs.

$$\begin{Bmatrix} \sigma_{xx} \\ \tau_{xn} \\ \tau_{xs} \end{Bmatrix} = \begin{bmatrix} E(n) & 0 & 0 \\ 0 & \frac{E(n)}{2(1+\nu)} & 0 \\ 0 & 0 & \frac{E(n)}{2(1+\nu)} \end{bmatrix} \begin{Bmatrix} \varepsilon_{xx} \\ \gamma_{xn} \\ \gamma_{xs} \end{Bmatrix} \tag{6}$$

Where (σ_{xx}, τ_{xn}, τ_{xs}) and (ε_{xx}, γ_{xn}, γ_{xs}) are the stress and strain components, respectively.

3. Variational formulation

The equilibrium equations can be obtained by using the stationary conditions $\delta(U-W)=0$, where *U* and *W* are the respectively the strain energy and the external load work.
The variation of strain energy is

$$\delta U = \int_0^L \iint_f \left(\sigma_{xx}\delta\varepsilon_{xx} + \tau_{xy}\delta\gamma_{xy} + \tau_{xz}\delta\gamma_{xz}\right)dydzdx$$

$$+\int_0^L \iint_w \left(\sigma_{xx}\delta\varepsilon_{xx} + \tau_{xy}\delta\gamma_{xy} + \tau_{xz}\delta\gamma_{xz}\right)dydzdx \tag{7a}$$

In the above equation the subscripts *f* and *w* denote respectively the flange and web of the box beam.

Using Eq. (5), the following expression for δU is obtained:

$$\delta U = \int_0^L [N\delta u_0' + (M_{zc}\cos(\theta) - M_{yc}\sin(\theta) + M_{zh}\cos(\theta) - M_{yh}\sin(\theta))\delta v_0''$$

$$+(Nv_0' - M_{zh}\theta'\sin(\theta) - M_{yh}\theta'\cos(\theta) + V_y\cos(\theta) - V_z\sin(\theta))\delta v_0'$$

$$+\left(M_{zc}\sin(\theta) + M_{yc}\cos(\theta) + M_{zh}\sin(\theta) + M_{yh}\cos(\theta)\right)\delta w_0''$$

$$+(Nw_0' + M_{zh}\theta'\cos(\theta) - M_{yh}\theta'\sin(\theta) + V_y\sin(\theta) + V_z\cos(\theta))\delta w_0'$$

$$+\left(M_{yh}\sin(\theta) - M_{zh}\cos(\theta)\right)\delta\phi_y' + (M_{zh}\theta'\sin(\theta) + M_{yh}\theta'\cos(\theta) + V_z\sin(\theta) - V_y\cos(\theta))\delta\phi_y$$

$$+\left(-M_{zh}\sin(\theta) - M_{yh}\cos(\theta)\right)\delta\phi_z' + (M_{yh}\theta'\sin(\theta) - M_{zh}\theta'\cos(\theta) - V_y\sin(\theta)$$
$$- V_z\cos(\theta))\delta\phi_z$$

$$+B_\omega\delta\theta''$$

$$+(M_R\theta' + T_{sv} + M_{zh}\left(w_0' - \phi_z\right)\cos(\theta) - M_{zh}\left(v_0' - \phi_y\right)\sin(\theta) - M_{yh}\left(w_0' - \phi_z\right)\sin(\theta)$$

$$-M_{yh}\left(v_0' - \phi_y\right)\cos(\theta))\delta\theta'$$
$$+(M_{zh}\left(w_0'' - \phi_z'\right)\cos(\theta) - M_{zh}\left(v_0'' - \phi_y'\right)\sin(\theta) - M_{zh}\theta'\left(v_0' - \phi_y\right)\cos(\theta)$$
$$-M_{zh}\theta'\left(w_0' - \phi_z\right)\sin(\theta) - M_{yh}\left(w_0'' - \phi_z'\right)\sin(\theta) - M_{yh}\theta'\left(w_0' - \phi_z\right)\cos(\theta)$$
$$-M_{yh}\left(v_0'' - \phi_y'\right)\cos(\theta) + M_{yh}\theta'\left(v_0' - \phi_y\right)\sin(\theta) - V_y\left(v_0' - \phi_y\right)\sin(\theta)$$
$$+V_y\left(w_0' - \phi_z\right)\cos(\theta) - V_z\left(w_0' - \phi_z\right)\sin(\theta) - V_z\left(v_0' - \phi_y\right)\cos(\theta)$$
$$-M_{zc}(v_0''\,\sin(\theta) - w_0''\,\cos(\theta)) - M_{yc}(w_0''\,\sin(\theta) + v_0''\,\cos(\theta)))\delta\theta]dx \tag{7b}$$

The stress resultants are defined by integrating over the flange and web cross-sectional area as

$$N = \iint_f \sigma_{xx}dydz + \iint_w \sigma_{xx}dydz \tag{8a}$$

$$V_y = \iint_f \tau_{xy}\frac{df(y)}{dy}dydz + \iint_w \tau_{xy}\frac{df(y)}{dy}dydz \tag{8b}$$

$$V_z = \iint_f \tau_{xz}\frac{df(z)}{dz}dydz + \iint_w \tau_{xz}\frac{df(z)}{dz}dydz \tag{8c}$$

$$M_{zc} = -\iint_f y\sigma_{xx}dydz - \iint_w y\sigma_{xx}dydz \tag{8d}$$

$$M_{yc} = -\iint_f z\sigma_{xx}dydz - \iint_w z\sigma_{xx}dydz \tag{8e}$$

$$M_{zh} = \iint_f f(y)\sigma_{xx}dydz + \iint_w f(y)\sigma_{xx}dydz \tag{8f}$$

$$M_{yh} = \iint_f f(z)\sigma_{xx}dydz + \iint_w f(z)\sigma_{xx}dydz \tag{8g}$$

$$T_{sv} = \iint_f \tau_{xz}\left(y - \frac{\partial\psi}{\partial z}\right) - \tau_{xy}\left(z + \frac{\partial\psi}{\partial y}\right)dydz$$
$$+\iint_w \tau_{xz}\left(y - \frac{\partial\psi}{\partial z}\right) - \tau_{xy}\left(z + \frac{\partial\psi}{\partial y}\right)dydz \tag{8h}$$

$$B_\omega = -\iint_f \psi\sigma_{xx}dydz - \iint_w \psi\sigma_{xx}dydz \tag{8i}$$

$$M_R = \iint_f (y^2 + z^2)\sigma_{xx}dydz + \iint_w (y^2 + z^2)\sigma_{xx}dydz \tag{8j}$$

Where N is the axial forces, M_{yc} and M_{zc} are the bending moments, T_{sv} is the St-Venant torsion moment, B_ω is the bimoment and M_R is a higher order stress resultant. However, the appearance of the higher order moments M_{yh} and M_{zh} and the non-usual transverse shear forces V_y and V_z is due to the particular form of the displacement field Eq. (2a).

In the present study, the lateral buckling of beams initially in bending about the principal axis is considered. The applied loads are then reduced to the lateral distributed load on point P located on the section contour in Fig. 2(b). The external work variation is defined by the relationship

$$\delta W = \int_0^L q_y\delta v\,dx \tag{9}$$

From the above relationship for v, the following expression for δv and δW are obtained

$$\delta v = \delta v_0 - e_z\cos\theta\,\delta\theta - e_y\sin\theta\,\delta\theta \tag{10}$$

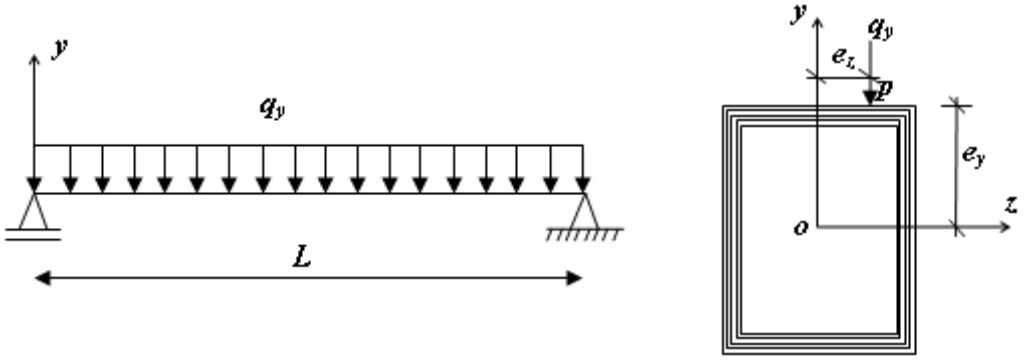

(a) (b)

Fig. 2 Simply supported beam under distributed load

$$\delta W = \int_0^L q_y \delta v_0 \, dx - \int_0^L q_y (e_z \cos + e_y \sin\theta)\delta\theta \, dx \tag{11}$$

3.1 Constitutive equations

Assuming that the edges are free in the axial sense (N=0), and after some calculations, the reduced constitutive equations with all elastic effects of FGM box beam may be expressed in the terms of stress resultants in the following form

$$\begin{Bmatrix} V_y \\ V_z \\ M_R \end{Bmatrix} = \begin{bmatrix} k_{22} & 0 & 0 \\ 0 & k_{33} & 0 \\ 0 & 0 & \bar{k}_{44} \end{bmatrix} \begin{Bmatrix} \gamma_y^0 \\ \gamma_z^0 \\ \frac{1}{2}\theta'^2 \end{Bmatrix} \tag{12a}$$

$$\begin{Bmatrix} M_{zc} \\ M_{zh} \\ M_{yc} \\ M_{yh} \\ T_{sv} \\ B_\omega \end{Bmatrix} = \begin{bmatrix} k_{66} & k_{67} & 0 & 0 & 0 & 0 \\ k_{76} & k_{77} & 0 & 0 & 0 & 0 \\ 0 & 0 & k_{88} & k_{89} & 0 & 0 \\ 0 & 0 & k_{98} & k_{99} & 0 & 0 \\ 0 & 0 & 0 & 0 & k_{55} & 0 \\ 0 & 0 & 0 & 0 & 0 & k_{10} \end{bmatrix} \begin{Bmatrix} \kappa_y \\ \gamma_y^{0\prime} \\ \kappa_z \\ \gamma_z^{0\prime} \\ \theta' \\ \theta'' \end{Bmatrix} \tag{12b}$$

Here, k_{ij} are stiffness coefficients of the FGM box beam. The explicit forms of k_{ij} are given in the Appendix.

The beam strain fields of the above equations, associated with the displacement fields are defined as

$$\varepsilon_0 = u_0' + \frac{1}{2}(v_0'^2 + w_0'^2) \tag{13a}$$

$$\gamma_y^0 = (\left(v_0' - \phi_y\right)\cos(\theta) + \left(w_0' - \phi_z\right)\sin(\theta)) \tag{13b}$$

$$\gamma_y^{0'} = (\left(v_0'' - \phi_y'\right)\cos(\theta) - \theta'\left(v_0' - \phi_y\right)\sin(\theta) + \left(w_0'' - \phi_z'\right)\sin(\theta) + \theta'\left(w_0' - \phi_z\right)\cos(\theta) \tag{13c}$$

$$\gamma_z^0 = \left(\left(w_0^{'} - \phi_z\right)\cos(\theta) - \left(v_0^{'} - \phi_y\right)\sin(\theta)\right) \tag{13d}$$

$$\gamma_z^{0'} = \left(\left(w_0^{''} - \phi_z^{'}\right)\cos(\theta) - \theta^{'}\left(w_0^{'} - \phi_z\right)\sin(\theta) - \left(v_0^{''} - \phi_y^{'}\right)\sin(\theta) - \theta^{'}\left(v_0^{'} - \phi_y\right)\cos(\theta)\right) \tag{13e}$$

$$\kappa_y = v_0^{''}\cos(\theta) + w_0^{''}\sin(\theta) \tag{13f}$$

$$\kappa_z = w_0^{''}\cos(\theta) - v_0^{''}\sin(\theta) \tag{13g}$$

3.2 Governing post-buckling equations

Governing equations of the present study can be established by using expressions of the strain energy (Eq. (7)) and external load work (Eq. (11)). The equilibrium equations can be rearranged and once integrated by parts it writes

$$\delta v_0: (M_{zc}\cos(\theta) - M_{yc}\sin(\theta) + M_{zh}\cos(\theta) - M_{yh}\sin(\theta))''$$
$$-(V_y\cos(\theta) - V_z\sin(\theta) - M_{zh}\theta'\sin(\theta) - M_{yh}\theta'\cos(\theta))' = q_y \tag{14a}$$

$$\delta w_0: \left(M_{zc}\sin(\theta) + M_{yc}\cos(\theta) + M_{zh}\sin(\theta) + M_{yh}\cos(\theta)\right)''$$
$$-(M_{zh}\theta'\cos(\theta) - M_{yh}\theta'\sin(\theta) + V_y\sin(\theta) + V_z\cos(\theta))' = 0 \tag{14b}$$

$$\delta\theta: B_\omega'' - (M_R\theta' + T_{sv} + M_{zh}(\gamma_z^0) - M_{yh}(\gamma_y^0))' + M_{zh}(\gamma_z^{0\prime}) - M_{yh}(\gamma_y^{0\prime}) + V_y(\gamma_z^0) - V_z(\gamma_y^0)$$
$$+M_{zc}(\kappa_z) - M_{yc}\left(\kappa_y\right) = -q_y(e_z\cos + e_y\sin\theta) \tag{14c}$$

$$\delta\phi_y: -\left(M_{yh}\sin(\theta) - M_{zh}\cos(\theta)\right)' + (M_{zh}\theta'\sin(\theta) + M_{yh}\theta'\cos(\theta) + V_z\sin(\theta) -$$
$$V_y\cos(\theta)) = 0 \tag{14d}$$

$$\delta\phi_z: \left(M_{zh}\sin(\theta) + M_{yh}\cos(\theta)\right)'\delta\phi_z' + (M_{yh}\theta'\sin(\theta) - M_{zh}\theta'\cos(\theta) - V_y\sin(\theta) -$$
$$V_z\cos(\theta) = 0 \tag{14e}$$

3.3 Lateral-torsional buckling loads

In the case of simply supported beams, the displacements are approximated by means of the following functions, which are compatible with the governing equations and the boundary conditions of the beam.

$$\{v_0, w_0, \theta, \phi_y, \phi_z\} = \{v_1 \sin(\pi x/L), w_1 \sin(\pi x/L), \theta_1 \sin(\pi x/L), \phi_{y1} \cos(\pi x/L), \phi_{z1} \cos(\pi x/L)\} \tag{15}$$

Where v_1, w_1, θ_1, ϕ_{y1} and ϕ_{z1} are the associated displacement amplitudes.
In order to solve the non-linear differential equations (Eq. (14)), Galerkin's method is first applied with the following approximations.

$$\cos\theta = 1 - \theta^2/2 \tag{16a}$$

$$\sin\theta = \theta - \theta^3/6 \tag{16b}$$

Inserting Eqs. (15) and (16) in (14a) and (14d), and carrying out the integration along the beam

length at the fundamental state $\{v_0, w_0, \theta, \phi_y, \phi_z\}=\{v_0, 0, 0, \phi_y, 0\}$, we find the reduced expressions of v_1 and ϕ_{y1}.

Consequently, the tangent stiffness matrix $[K(q_y,e_y)]$ is formulated through the adoption of Newton-Raphson algorithm at the fundamental state in which the functions $v_1(q_y,e_y)$ and $\phi_{y1}(q_y,e_y)$ are introduced. The expressions of the elements $K(q_y,e_y)_{ij}$ are not presented here because of their length.

Once the tangent stiffness matrix is determined, the buckling loads can be obtained by requiring the singularity of the tangential matrix *Det* $([K(q_y,e_y)])=0$. This procedure leads to a non-linear algebraic problem for the critical loads. After some simplifications, the general expression for the critical moment of unshearable FGM beams (Model III) is arranged as

$$M_{cr} = \frac{C_1\pi^2 k_{88}}{L^2}\left[C_2 e_y \pm \sqrt{\left(C_2 e_y\right)^2 + \frac{k_{10}\left(1+\frac{k_{55}L^2}{\pi^2 k_{10}}\right)}{k_{88}}}\right] \tag{17a}$$

With the following coefficients C_1 and C_2 defined as

$$C_1 = \frac{3\pi^4}{8\sqrt{1024}\sqrt{1-\frac{k_{88}}{k_{66}}}} \tag{17b}$$

$$C_2 = \frac{3\pi^2}{2\sqrt{1024}\sqrt{1-\frac{k_{88}}{k_{66}}}} \tag{17c}$$

It clearly appears that in contrast to the case of isotropic beams, for the FGM beams the coefficients C_1 and C_2 depend not only on the geometric ratio I_y/I_z but also on material properties. Note that the lengthy expressions of the critical moments for shearable beams (Model I and Model II), are not given here due to space limitations.

4. Results and discussions

In order to demonstrate the correctness and accuracy of the proposed model, Lateral-torsional buckling of both thin and thick-walled FGM box beams is studied. The geometric dimensions of the beams are tabulated in Table 1.

The beam walls are taken to be made of aluminum and alumina with the following material properties: Ceramic (alumina, Al2O3): $E_t=E_c$=380 GPa, v=0.3. Metal (aluminum, Al): $E_b=E_m$=70 GPa, v=0.3.

The variations in lateral buckling moments of FGM box beams for different power law indices (p) and different length are given in this section.

Table 1 Geometry of the beams

Parameters	Thin-walled beam	Thick-walled beam
d (mm)	24.200	106.700
c (mm)	13.600	50.800
h (mm)	0.762	15.240

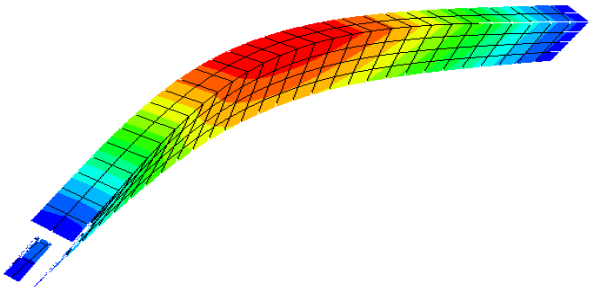

Fig. 3 Lateral-Buckling mode of thick-walled beams under distributed load for p=0.2 and L=1.524 m by ABAQUS simulation

Table 2 Buckling moments M_{cr} (in N.m) for thin-walled box beams, load on top

p	Method	L=0.321 m	L=0.521 m	L=0.721 m
Ceramic	Present	8434.35	5386.74	3951.36
	Abaqus	8239.35	5373.07	4085.61
0.2	Present	7471.48	4771.06	3499.27
	Abaqus	7389.29	4828.29	3553.02
1	Present	5254.02	3355.81	2461.34
	Abaqus	5160.41	3372.17	2484.95
10	Present	2299.29	1468.52	1077.05
	Abaqus	2255.01	1473.35	1085.83
Metal	Present	1553.69	992.31	727.91
	Abaqus	1517.78	989.78	752.61

Table 3 Buckling moments M_{cr} (in N.m) for thin-walled box beams, load on bottom

p	Method	L=0.321 m	L=0.521 m	L=0.721 m
Ceramic	Present	9731.79	5888.65	4214.96
	Abaqus	9876.89	5922.61	4230.89
0.2	Present	8606.63	5210.28	3729.95
	Abaqus	8475.81	5262.88	3741.69
1	Present	6053.66	3665.33	2623.91
	Abaqus	5917.81	3674.95	2616.78
10	Present	2649.23	1603.96	1148.18
	Abaqus	2585.86	1605.60	1143.42
Metal	Present	1792.70	1084.77	776.47
	Abaqus	1819.44	1091.01	779.37

Moreover, the effect of the height parameter (e_y) on the lateral buckling resistance is investigated by using a simply supported beam loaded on top and bottom flange.

The thin and thick-walled FGM box beams are modeled using ABAQUS software (C3D8 element type) with forty eight elements through the thickness (see Fig. 3). By (7488, 11520, 23040) and (9792, 11520, 17280) we define the total number of elements of the thin and thick-

walled beam associated with the beam lengths (0.321 m, 0.521 m, 0.721 m) and (1.124 m, 1.324 m, 1.524 m), respectively.

Based on Model (I), the lateral buckling moments of the thin-walled FGM box beams are computed for different values of power law indices *p*. The numerical results are displayed in Tables 2-3, along with the numerical solutions of finite element simulation.

It can be seen from the comparison shown in Tables 2-3 that the present results agree very well with the numerical solutions of ABAQUS analysis, these tables also show that the material distribution (*p*) and beam lengths are inversely proportional to critical moment, as expected.

The results predicted by the present model for thick-walled box beams are listed in Tables 4-5, they show a reasonable agreement with the values of ABAQUS analysis. The comparison in Table 4 indicates that the maximum relative error of the buckling moment obtained for L=1.324m and *p*=10 is about 6%.

The results in Tables 2-5 show that the beam resistance to lateral buckling is at greatest when the loads are applied on bottom flange.

It can be observed from Figs. 4-5 that the material distribution (*p*) has a significant effect on the lateral-buckling moments of the short thick and thin-walled box beams for the two load heights, this effect is much more significant for the short thin-walled box beams, whereas long beams reveal a much lower sensitivity to this effect. The same figures show that with the decrease of the

Table 4 Buckling moments M_{cr} (in N.m) for thick-walled box beams, load on top

P	Method	*L*=1.124 m	*L*=1.324 m	*L*=1.524 m
Ceramic	Present	1555118.08	1336705.28	1171843.17
	Abaqus	1578189.97	1359789.27	1112680.99
0.2	Present	1370267.89	1178517.66	1033616.60
	Abaqus	1437588.73	1238880.03	1016110.22
1	Present	1064530.26	916144.01	803854.19
	Abaqus	1104136.11	951986.06	784692.27
10	Present	527417.78	453541.77	370341.23
	Abaqus	496065.82	427573.68	352926.72
Metal	Present	286469.04	246235.20	206660.08
	Abaqus	290719.50	250487.61	204966.77

Table 5 Buckling moments M_{cr} (in N.m) for thick-walled box beams, load on bottom

P	Method	*L*=1.124 m	*L*=1.324 m	*L*=1.524 m
Ceramic	Present	1555118.08	1336705.28	1171843.17
	Abaqus	1578189.97	1359789.27	1112680.99
0.2	Present	1370267.89	1178517.66	1033616.60
	Abaqus	1437588.73	1238880.03	1016110.22
1	Present	1064530.26	916144.01	803854.19
	Abaqus	1104136.11	951986.06	784692.27
10	Present	527417.78	453541.77	370341.23
	Abaqus	496065.82	427573.68	352926.72
Metal	Present	286469.04	246235.20	206660.08
	Abaqus	290719.50	250487.61	204966.77

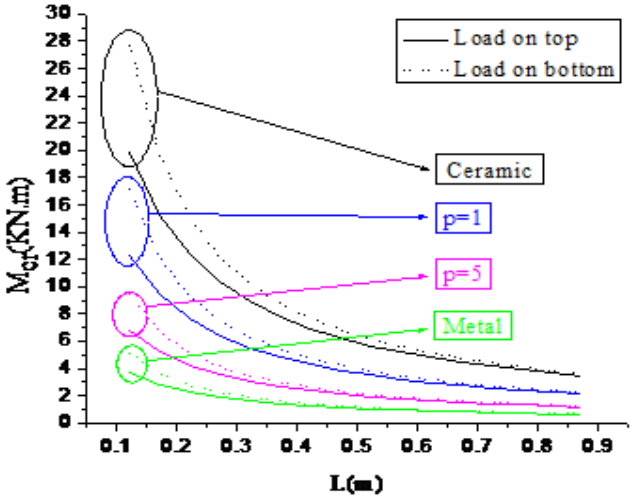

Fig. 4 Buckling moments vs length of thin-walled box beams

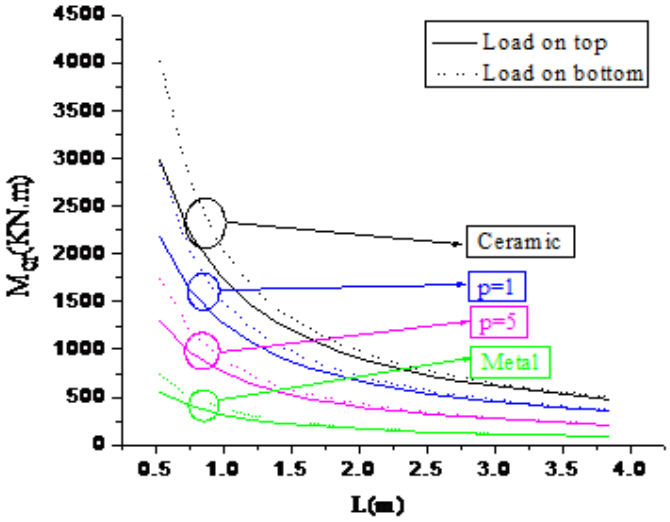

Fig. 5 Buckling moments vs length of thick-walled box beams

beam length, the differences between the top and bottom loads tend to increase.

Fig. 6 shows the critical moments vs cross-section ratio (*c/d*) for different values of power law indices *p*. it is seen that these moments are proportional to cross-section ratio. Moreover, in contrast to the case of beams with small flanges, the differences between the top and bottom loads become very important for large flanges.

Effect of the material distribution on the lateral buckling moments of FGM box beams with respect to thickness-to-side ratio (*h*/*d*) variation is displayed in Fig. 7. This plot reveals that the material distribution (*p*) has a significant effect on the thick beams (this effect becomes greater when the load is applied to the bottom flange).

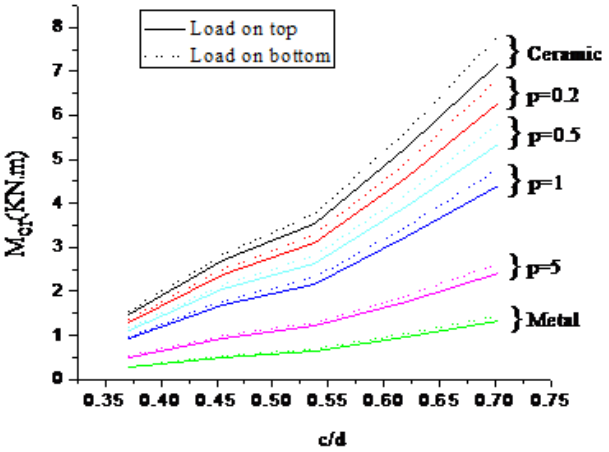

Fig. 6 Buckling moments vs cross-section ratio *c/d* for *h*=0.000762 m for *L*=0.721 m

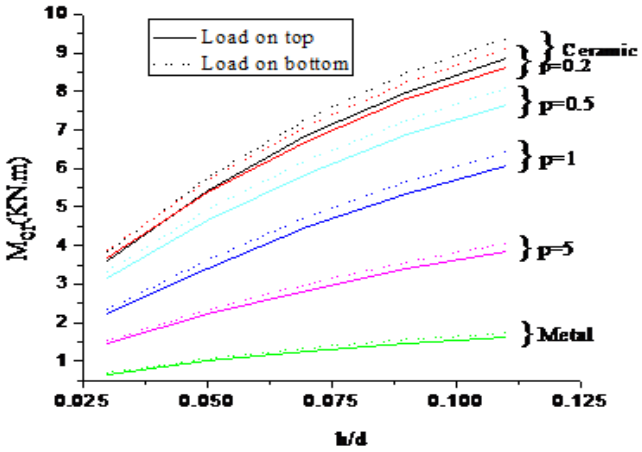

Fig. 7 Buckling moments vs thickness-to-side ratio (*h*/*d*) for *c*=0.0136 m and *L*=0.762 m

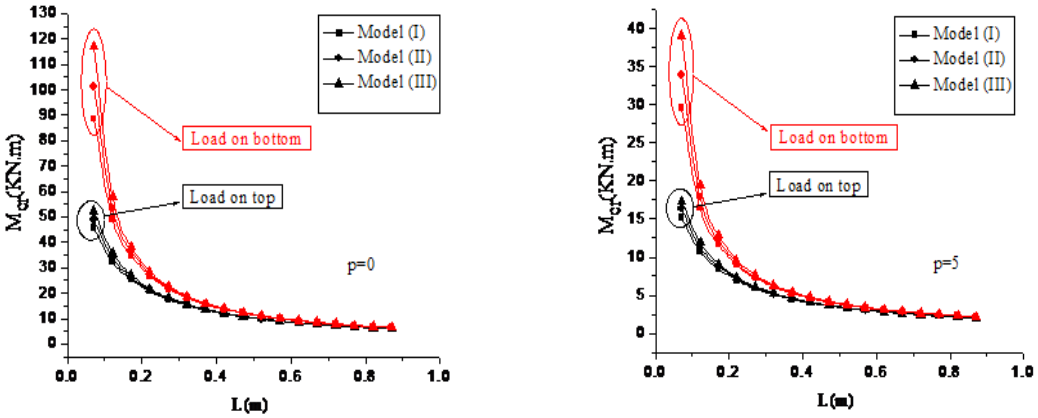

(a) (b)

Fig. 8 Buckling moments vs lengths (*L*) for *d*=0.0242 m, *c*=0.017 m and *h*=0.000762 m

Table 6 buckling moments (M_{cr} in KN.m) for h=0.000762 m and L=0.121 m

P	Model	c/d=0.70		c/d=0.54		c/d=0.37	
		Top	Bottom	Top	Bottom	Top	Bottom
Ceramic	(I)	32.145	49.137	16.951	23.771	7.537	10.055
	(II)	33.952	53.486	17.692	25.256	7.733	10.408
	(III)	35.803	58.071	18.323	26.508	7.874	10.647
0.2	(I)	28.041	42.866	14.813	20.775	6.612	8.821
	(II)	29.648	46.705	15.484	22.103	6.800	9.150
	(III)	31.248	50.704	16.023	23.191	6.913	9.351
0.5	(I)	23.874	36.500	12.637	17.724	5.664	7.556
	(II)	25.251	39.790	13.216	18.871	5.829	7.845
	(III)	26.620	43.214	13.679	19.806	5.927	8.020
1	(I)	19.545	29.927	10.333	14.524	4.678	6.244
	(II)	20.661	32.625	10.799	15.463	4.765	6.436
	(III)	21.803	35.468	11.192	16.249	4.899	6.635
5	(I)	10.733	16.411	5.757	8.054	2.571	3.433
	(II)	11.261	17.804	6.026	8.582	2.649	3.569
	(III)	11.977	19.456	6.240	9.014	2.694	3.650
Metal	(I)	5.922	9.051	3.122	4.379	1.388	1.852
	(II)	6.254	9.853	3.259	4.652	1.425	1.917
	(III)	6.595	10.697	3.375	4.883	1.450	1.961

Fig. 8 shows the influence of shear deformation on the critical moments of FGM box beam for p=0, 5; the minimum M_{cr} occurs for the Model (I), the maximum for the Model (III), the intermediate one for the Model (II). These results confirm that the unshearable model is conservative.

It is interesting to note that the shear effect is negligibly small for the long beams, especially for structures loaded on top flanges, but for short beams the difference between Model (I) and Model (III) is very impressive and can reach 25%.

This effect is further illustrated in Table 6, which shows that for different values of p, the beams with small flanges are very little influenced by transverse shear. With the increase of the cross-section ratio c/d, the lateral buckling moments are more and more influenced by this effect. The difference between the Model (I) and Model (III) results is significant (16%) for c/d=0.7.

5. Conclusions

In this study, attention is focused on the analysis of lateral-torsional buckling for simply supported thick and thin-walled FGM box beams under uniformly distributed loads. The properties of the assumed beams vary in the wall thickness direction according to power law. The final form of the tangential matrix is obtained by employing Galerkin's technique and then solved after applying appropriate boundary conditions. The new proposed non-linear kinematical model, depend basically on the non-classical effects such as the primary and secondary warping and the transverse shear.

From this analysis, following conclusions are drawn:

1. A general expression for the buckling moment of unshearable FGM beams has been proposed.
2. The results obtained by the present method are in excellent agreement with those of ABAQUS simulation.
3. The present model is applicable to both thin and thick-walled FGM box beams.
4. The results reveal that the transverse shear effect is important for the short beams and/or high cross-section ratios. They also confirm that the unshearable model is conservative.

References

Abaqus standard user's manual version 6.4. (2003), *Hibbit*, Karlsson and Sorensen Inc., Pawtucket, RI, USA.

Ait Amar Meziane, M., Abdelaziz, H.H. and Tounsi, A. (2014), "An efficient and simple refined theory for buckling and free vibration of exponentially graded sandwich plates under various boundary conditions", *J. Sandw. Struct. Mater.*, **16**(3), 293-318.

Ait Yahia, S., Ait Atmane, H., Houari, M.S.A. and Tounsi, A. (2015), "Wave propagation in functionally graded plates with porosities using various higher-order shear deformation plate theories", *Struct. Eng. Mech.*, **53**(6), 1143-1165.

Al-Basyouni, K.S., Tounsi, A. and Mahmoud, S.R. (2015), "Size dependent bending and vibration analysis of functionally graded micro beams based on modified couple stress theory and neutral surface position", *Compos. Struct.*, **125**, 621-630.

Belabed, Z., Houari, M.S.A., Tounsi, A., Mahmoud, S.R. and Anwar Bég, O. (2014), "An efficient and simple higher order shear and normal deformation theory for functionally graded material (FGM) plates", *Compos. Part B*, **60**, 274-283.

Bouderba, B., Houari, M.S.A. and Tounsi, A. (2013), "Thermomechanical bending response of FGM thick plates resting on Winkler-Pasternak elastic foundations", *Steel Compos. Struct.*, **14**, 85-104.

Bourada, M., Kaci, A., Houari, M.S.A. and Tounsi, A. (2015), "A new simple shear and normal deformations theory for functionally graded beams", *Steel Compos. Struct.*, **18**(2), 409-423.

Bousahla, A.A., Houari, M.S.A., Tounsi, A. and Adda Bedia, E.A. (2014), "A novel higher order shear and normal deformation theory based on neutral surface position for bending analysis of advanced composite plates", *Int. J. Comput. Meth.*, **11**(6), 1350082.

Cortínez, V.H. and Piovan, M.T. (2002), "Vibration and buckling of composite thin walled beams with shear deformability", *J Sound Vib.*, **258**(4), 701-23.

Dung, D.V. and Hoa, L.K. (2013), "Research on nonlinear torsional buckling and post-buckling of eccentrically stiffened functionally graded thin circular cylindrical shells", *Compos. Part B*, **51,** 300-309.

Erkmen, R.E. (2014), "Shear deformable hybrid finite-element formulation for buckling analysis of thin-walled members", *Finite Elem. Anal. Des.*, **82**, 32-45.

Erkmen, R.E. and Attard, M.M. (2011), "Lateral-torsional buckling analysis of thin-walled beams including shear and pre-buckling deformation effects", *Int. J. Mech. Sci.*, **53**, 918-925.

Fraternali, F. and Feo, L. (2000), "On a moderate rotation theory of thin-walled composite beams", *Compos. Part B*, **31**, 141-58.

Fekrar, A., Houari, M.S.A., Tounsi, A. and Mahmoud, S.R. (2014), "A new five-unknown refined theory based on neutral surface position for bending analysis of exponential graded plates", *Meccanica*, **49**, 795-810.

Fu, C.C and Hsu, Y.T. (1995), "The development of an improved curvilinear thin-walled Vlasov element", *Comput. Struct.*, **54**, 147-159.

Gjelskin, A. (1981), *The Theory of Thin-Walled Bars*, John Wiley an Sons Inc, New York, USA.

Gonçalves, R. (2012), "A geometrically exact approach to lateral-torsional buckling of thin-walled beams with deformable cross-section", *Comput. Struct.*, **106-107**, 9-19.
Hebali, H., Tounsi, A., Houari, M.S.A., Bessaim, A. and Adda Bedia, E.A. (2014), "New quasi-3D hyperbolic shear deformation theory for the static and free vibration analysis of functionally graded plates", *J. Eng. Mech.*, ASCE, **140**, 374-383.
Khalfi, Y., Houari, M.S.A. and Tounsi, A. (2014), "A refined and simple shear deformation theory for thermal buckling of solar functionally graded plates on elastic foundation", *Int. J. Comput. Meth.*, **11**(5), 135007.
Kim, N.I., Shin, D.K. and Kim, M.Y. (2008), "Flexural-torsional buckling loads for spatially coupled stability analysis of thin-walled composite columns", *Adv. Eng. Softw.*, **39**, 949-961.
Kim, Y.Y. and Kim J.H. (1999), "Thin-walled closed box element for static and dynamic analysis", *Int. J. Numer. Meth. Eng.*, **45**, 473-490.
Lanc, D., Vo, T.P., Turkalj, G. and Lee, J. (2015), "Buckling analysis of thin-walled functionally graded sandwich box beams", *Thin Wall. Struct.*, **86**, 148-156.
Lofrano, E., Paolone, A. and Ruta, G. (2013), "A numerical approach for the stability analysis of open thin-walled beams", *Mech. Res. Commun.*, **48**, 76- 86.
Machado, S.P. and Cortínez, V.H. (2005), "Lateral buckling of thin-walled composite bisymmetric beams with prebuckling and shear deformation", *Eng. Struct.*, **27**, 1185-1196.
Machado, S.P. and Cortínez, V.H. (2005), "Non-linear model for thin-walled composite beams with shear deformation", *Thin Wall. Struct.*, **43**, 1615-1645.
Mohri, F., Azrar, L. and Potier-Ferry, M. (2002), "Lateral post-buckling analysis of thin-walled open section beams", *Thin Wall. Struct.*, **40**, 1013-1036.
Paulsen, F. and Welo, T. (2001), "Cross-sectional deformations of rectangular hollow sections in bending. Part II-Analytical models", *Int. J. Mech. Sci.*, **43**, 131-152.
Pignataro, M., Rizzi, N., Ruta, R. and Varano. V. (2010), "The effects of warping constraints on the buckling of thin-walled structures", *J. Mech. Mater. Struct.*, **4**(10), 1711-1727.
Ruta, G.C., Varano, V., Pignataro, M. and Rizzi, L.R. (2008), "A beam model for the flexural-torsional buckling of thin-walled members with some applications", *Thin Wall. Struct.*, **46**(7), 816-822.
Sapkàs, A. and kollàr, L.P. (2002), "Lateral-torsional buckling of composite beams", *Int. J. Solid. Struct.*, **39**, 2939-2963.
Shen, H. (2009), "Torsional buckling and postbuckling of FGM cylindrical shells in thermal environments", *Int. J. Nonlin. Mech.*, **44**, 644-657.
Sokolnikoff, I.S. (1946), *Mathematical Theory of Elasticity*, McGraw-Hill, New York, USA.
Reddy, J.N. (1984), "A simple higher-order theory for laminated composite plates, *J. Appl. Mech.*, **51**, 745-752.
Tounsi, A., Houari, M.S.A., Benyoucef, S. and Adda Bedia, E.A. (2013), "A refined trigonometric shear deformation theory for thermoelastic bending of functionally graded sandwich plates", *Aerosp. Sci. Tech.*, **24**, 209-220.
Vlasov, V.Z. (1962), *Thin Walled Elastic Beams*, Moscow, French Translation, Pieces Longues en Voiles Minces, Eyrolles, Paris, France.
Wakashima, K., Hirano, T. and Niino, M. (1990), "Functionally gradient materials (FGM) architecture: a new type of ceramic/metal assemblage designed for hot structural components », *Space Applications of Advanced Structural Materials*, Noordwijk, March.
Ziane, N., Meftah, S.A., Belhadj, H.A., Tounsi, A. and Bedia, E.A. (2013), "Free vibration analysis of thin and thick-walled FGM box beams", *Int. J. Mech. Sci.*, **66**, 273-282.
Zidi, M., Tounsi, A., Houari, M.S.A., Adda Bedia, E.A. and Anwar Bég, O. (2014), "Bending analysis of FGM plates under hygro-thermo-mechanical loading using a four variable refined plate theory", *Aerosp. Sci. Tech.*, **34**, 24-34.

Appendix

$$k_{11} = \iint_s E(n)dydz$$

$$k_{14} = k_{41} = \iint_s E(n)(y^2 + z^2)dydz$$

$$k_{22} = \iint_s \frac{E(n)}{2(1+\nu)}\left(\frac{df(y)}{dy}\right)^2 dydz$$

$$k_{33} = \iint_s \frac{E(n)}{2(1+\nu)}\left(\frac{df(z)}{dz}\right)^2 dydz$$

$$k_{44} = \iint_s E(n)(y^2 + z^2)^2 dydz$$

$$k_{55} = \iint_s \frac{E(n)}{2(1+\nu)}\left(\left(y - \frac{\partial\psi}{\partial z}\right)^2 + \left(z + \frac{\partial\psi}{\partial y}\right)^2\right)dydz$$

$$k_{66} = \iint_s E(n)y^2 dydz$$

$$k_{67} = k_{76} = -\iint_s E(n)yf(y)dydz$$

$$k_{77} = \iint_s E(n)f(y)^2 dydz$$

$$k_{88} = \iint_s E(n)z^2 dydz$$

$$k_{89} = k_{98} = -\iint_s E(n)zf(z)dydz$$

$$k_{99} = \iint_s E(n)f(z)^2 dydz$$

$$k_{10} = \iint_s E(n)\psi^2 dydz$$

$$\bar{k}_{44} = k_{44} - \frac{k_{14}k_{41}}{k_{11}}$$